Computer Methods and Advance[illegible]echanics, Siriwardane & Zaman (eds)
©[illegible]ema, Rotterdam, ISBN 90 5410 380 9

Selective reduced integration in numerical model[illegible] soil plasticity

F.B.Mok
Department of Engineering, University of Manchester, UK
D.V.Griffiths
Department of Engineering, Colorado School of Mines, Colo., USA

ABSTRACT: The paper describes some results obtained using selective reduced integration (SRI) in numerical modelling of soil plasticity. Included in this discussion will be the effect of various splitting techniques on the deviatoric and volumetric components of the constitutive model. A backward Euler method is used in the elasto-plastic rate integration. Bearing capacity problems for both cohesive and frictional soils have been used as a basis of comparison.

1 INTRODUCTION

The ultimate bearing capacity of a soil mass can be estimated numerically using the finite element method. In two-dimensions, Zienkiewicz et al[1] and Griffiths[2] used 8-node quadrilaterals with reduced integration to determine the bearing capacity of cohesive and frictional soils. For those who advocated full integration, Sloan and Randolph[3] used 15-node triangles in predicting collapse loads of undrained cohesive soils which was extended to frictional soils by de Borst and Vermeer[4]. The use of simpler elements such as the 4-node quadrilateral was described by Prevost and Hughes[5], however little has been reported on the use of these elements with frictional soils. As there is a good case for using elements that are no more complicated than necessary in the analysis of plasticity problems in geomechanics, the present work studies the effectiveness of linear quadrilaterals in the analysis of bearing capacity and also extrapolates some of the observations made to 3-d problems.

The limitations of linear quadrilaterals in limit load evaluations were discussed by Nagtegaal et al[6]. The limit load tends to be too high with a full integration scheme whereas a uniformly reduced integration scheme is susceptible to the formation of zero energy modes. One of the alternatives is to adopt a selective integration scheme in which different orders of integration are applied to the deviatoric and volumetric components (e.g. Hughes[7]). The deviatoric component is fully integrated while the volumetric component is under integrated. This technique has been used with success in cohesive soils[5] in which yielding is pressure independent and there is zero plastic volume change. Its application to pressure sensitive or frictional soil models is discussed in this paper.

2 SPLITTING THE ELASTIC MATRIX

In selective integration, the elastic matrix $(\mathbf{D})$ is split into its deviatoric and volumetric components. Two different splits[8] are possible of the type; λ, μ and G, K. The elastic matrix in plane strain is:

$$D = \begin{bmatrix} 2\mu & 0 & 0 & 0 \\ 0 & 2\mu & 0 & 0 \\ 0 & 0 & \mu & 0 \\ 0 & 0 & 0 & 2\mu \end{bmatrix} + \begin{bmatrix} \lambda & \lambda & 0 & \lambda \\ \lambda & \lambda & 0 & \lambda \\ 0 & 0 & 0 & 0 \\ \lambda & \lambda & 0 & \lambda \end{bmatrix} \tag{1}$$

where

$$\mu = \frac{E}{2(1+\nu)}\ ,\ \lambda = \frac{E\nu}{(1-2\nu)(1+\nu)} \tag{2}$$

and

$$D = \frac{1}{3}\begin{bmatrix} 4G & -2G & 0 & -2G \\ -2G & 4G & 0 & -2G \\ 0 & 0 & 3G & 0 \\ -2G & -2G & 0 & 4G \end{bmatrix} + \begin{bmatrix} K & K & 0 & K \\ K & K & 0 & K \\ 0 & 0 & 0 & 0 \\ K & K & 0 & K \end{bmatrix} \tag{3}$$

where

$$G = \frac{E}{2(1+\nu)}\ ,\ K = \frac{E}{3(1-2\nu)} \tag{4}$$

Full integration (2 by 2) is applied to the first term while the second term is formed using reduced integration (1 by 1). The first method of splitting the elastic matrix leads to a diagonal deviatoric matrix, whereas the second method leads to a more fully populated deviatoric matrix. The latter method is arguably a more 'natural' split in that the familiar shear and bulk moduli are clearly separated.

3 ELASTO-PLASTIC RATE INTEGRATION

A backward Euler method is applied to integrate the elasto-plastic incremental equations. This method has been shown to be numerically stable, and allows large load steps to be applied without loss of accuracy in materials with von Mises or Tresca yield criteria[9]. An incremental elastic stress is initially predicted, which is added to the stress already existing at that location. If the resultant trial stress is found to violate the yield criterion, a plastic stress is determined and applied to ensure the resultant stress lies on the yield surface. Let σ_o be the stress at the start of a step, $\Delta\sigma_e$ be the incremental elastic stress, σ_e be the trial stress and $\Delta\sigma$ be the corrected stress.

$$\sigma_e = \sigma_o + \Delta\sigma_e \tag{5}$$

$$\Delta\sigma = \Delta\sigma_e - < \lambda > D\frac{\partial g}{\partial \sigma} \tag{6}$$

where λ is a plastic multiplier, and $\frac{\partial g}{\partial \sigma}$ is derivative of the plastic potential.

The bracket <> is introduced as an operator with the meaning that only positive values are considered. The corrected stress can be deviatoric or hydrostatic, depending on the elastic matrix used. The plastic multiplier is found by linearising the yield function at σ_e and equating it to zero. For an elastic perfectly plastic material, the plastic multiplier is

$$\lambda = \frac{f(\sigma_e)}{(\frac{\partial f}{\partial \sigma})^T D(\frac{\partial g}{\partial \sigma})} \tag{7}$$

and

$$\frac{\partial f}{\partial \sigma} = \frac{\partial g}{\partial \sigma} \tag{8}$$

for an associated flow.

A two vector correction[10,11] is applied when the corrected stress crosses the corners of a Mohr Coulomb yield criterion.

4 ANALYSES

Results for a weightless soil without surcharge are now presented. Both cohesive and frictional soils are considered and the finite element meshes consist of 4-node plane strain elements in 2-d and 8-node bricks in 3-d. In the latter case, a 'skyline' profile is adopted (see e.g. Smith and Griffiths[12]). It was found that this strategy not only saved on memory requirements, but also ran faster as well. An 'initial stress' approach is used in which all the iterations employed a constant global stiffness matrix (modified Newton-Raphson). The number of Gauss points is the same in both the stiffness and plastic stress re-distribution phases of the calculation. The mesh is incrementally loaded until failure is indicated by a sudden increase in displacements. This failure condition is usually confirmed by an inability of the numerical procedure to converge in the prescribed maximum number of iterations.

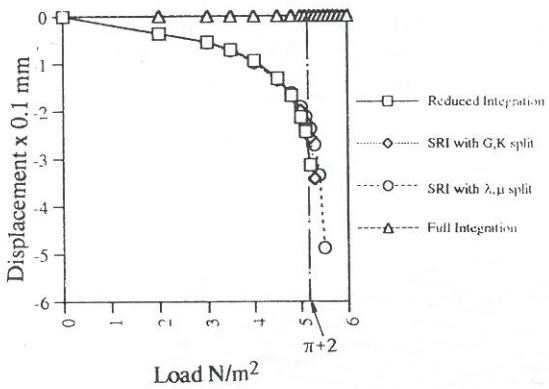

Figure 1. Load displacement curves for a cohesive soil with $\nu \approx 0.5$.

5 RESULTS

Load displacement curves of the cohesive soil from $\nu \approx 0.5$ is shown in Figure 1. The theoretical limit load, $N_c = 5.14$, is compared with the results from the different integration schemes. The reduced integration gives very good agreement, however under scrutiny the mesh suffers from hourglassing as shown in Figure 2. The SRI scheme with G, K split performs marginally better than the λ,μ split, although the difference decreases at high Poisson ratio (Table 1). All the subsequent SRI analyses use a G, K split. The locking phenomenon is clearly shown in the mesh which uses full integration.

Table 1. Limit loads of the cohesive soil with different Poisson's ratios.

	$.0 < \nu \leq .3$	$.3 < \nu < .5$
λ,μ split	5.6	5.5
G,K split	5.3	5.3

In the analyses with a Mohr Coulomb yield criterion, it is noted that the out-of-plane stress is not always equal to the intermediate principal stress. This anomaly was most frequently observed when using a Tresca yield criterion with low Poisson's ratios and was more widespread when using non-associated flow rules as opposed to associated flow rules. It was observed that for Poisson's ratios equal to 0.3 or higher, the problem was not widespread throughout the mesh and did not have a significant influence on the global response. The remainder of the analyses presented in this paper used a Poisson's ratio of 0.3.

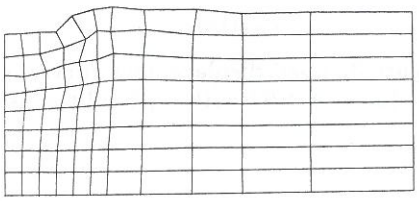

Figure 2. Deformed mesh of a cohesive soil with $\nu \approx 0.5$, reduced intergration is used.

Table 2. Limit loads of the C-ϕ soil (ϕ=ψ).

ϕ	Theory	Reduced integration	SRI with G, K split	Full integration
0°	5.1	5.2	5.4	5.9
5°	6.5	6.6	6.8	7.7
10°	8.3	8.5	8.7	10.0
20°	14.8	14.8	15.4	17.0
30°	30.1	28.8	30.0	41.0
35°	46.1	38.7	43.5	56.8
40°	75.3	56.1	66.5	78.3

The limit loads of the cohesive and frictional soil with an associated flow rule are detailed in Table 2. Although reduced integration only has a single point of constitutive equation calculation, it suffers from hourglassing. Also, the limit load is underestimated when the friction angle is greater than twenty degrees. In general, the agreement between the theory and the SRI scheme is reasonable, though it deteriorates at high friction angle where $\phi > 30^o$. Full integration always resulted in limit loads higher than theory, a result not welcomed by engineers.

The limit loads of the cohesive and frictional soils with non-associated flows are reported in Table 3. The load displacement curves for $\phi = 30^o$ are shown in Figure 3. The results from the non-associated flow are less satisfactory, especially with non-dilating soils. If the difference between the friction and dilation angle is kept within ten degrees ($\phi - \psi \not< 10^o$) better results are obtained. A similar observation was made by de Borst and Vermeer[4] and this result appears to be a product of the return algorithm. No such restriction on the value of

Table 3. Limit loads of the C-ϕ soil with different dilation angles.

ϕ	$\psi = 0^o$	$\psi = 10^o$	$\psi = 20^o$	$\psi = 30^o$
10^o	8.7	8.7		
20^o	14.5	15.3	15.4	
30^o	21.0	27.0	30.0	30.0

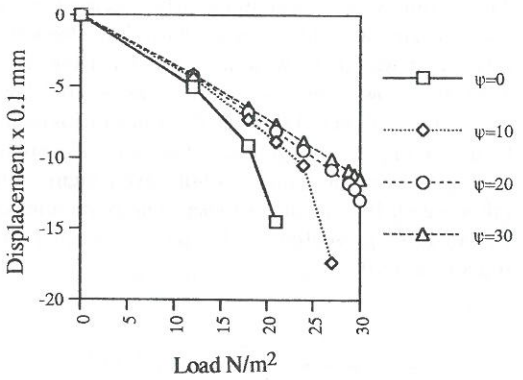

Figure 3. Load displacement curves of a C-ϕ soil (ϕ=30°), SRI with G,K split is used.

Table 4. Limit loads of the C-ϕ soil from 3-d analyses.

ϕ	Theory	ϕ=ψ	ψ=0
von Mises	6.2	6.9	
0^o	6.2	6.6	
5^o	8.5	8.9	8.7
10^o	10.0	11.6	10.5
20^o	17.8	20.8	18.8
30^o	36.1	38.5	33.8
35^o	55.3	61.6	46.6
40^o	90.4	55.0	73.5

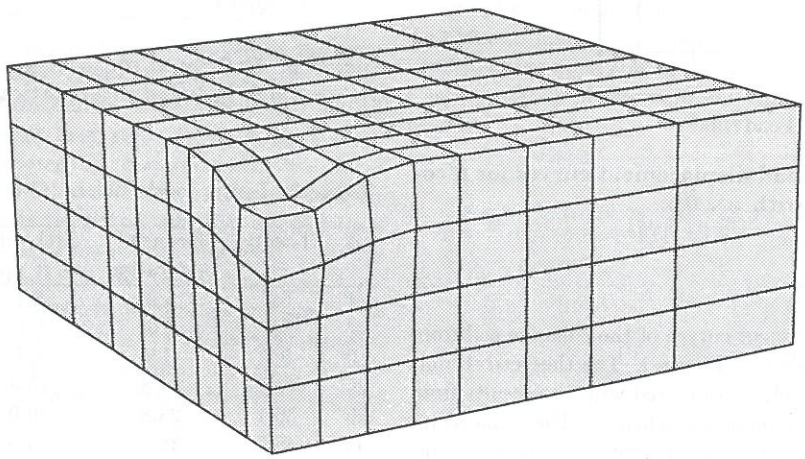

Figure 4. Deformed mesh of a cohesive soil with $\nu = 0.3$, SRI G, K.

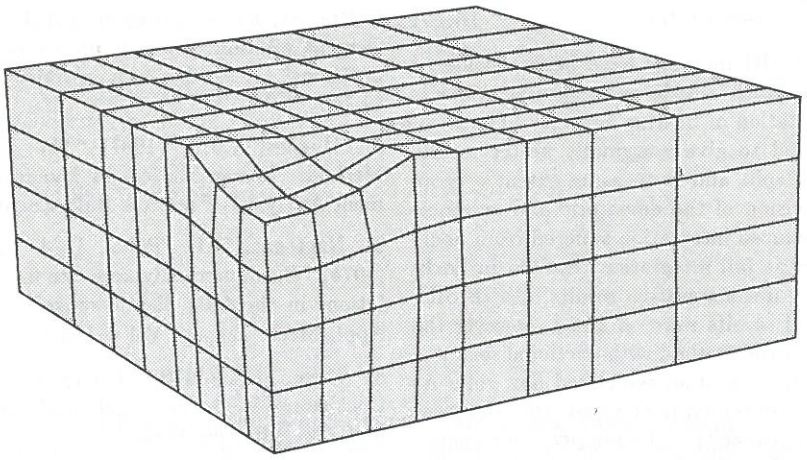

Figure 5a. Deformed mesh of a $c-\phi$ soil ($\phi = \psi = 30^o$), SRI G, K.

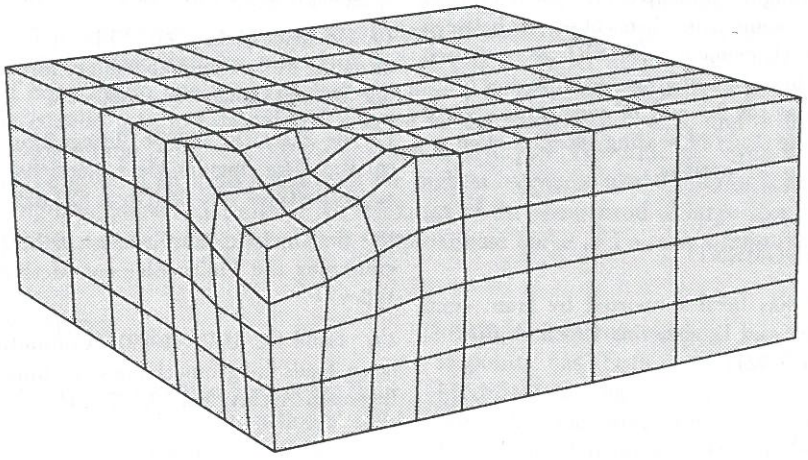

Figure 5b. Deformed mesh of a $c-\phi$ soil ($\phi = 30^o, \psi = 0^o$), SRI G, K.

ψ is observed when using the 'global' viscoplastic algorithm (see e.g. Griffiths[13]).

The deformed mesh of the cohesive soil with $\nu = 0.3$ is shown in Figure 4 while Figure 5 shows the deformed mesh with $\phi = 30^o$. The latter has a more diffused deformation than the former. The heave at the edge of the footing is more apparent in frictional soils.

Limit loads from the 3-d analyses are reported in Table 4. Large load steps are used to reduce the computing time (most of the analyses require only 5 load steps) and convergent solutions are obtained without excessive computing effort. Close agreement is observed between the theory and the finite element analyses for friction angle less than thirty. Limit loads from non dilating soils are slightly lower than those with associated plastic flow.

6 CONCLUSIONS

The backward Euler method used to integrate the elasto-plastic rate equations was found to be robust, with stable solutions obtained with relatively large load steps. The algorithm also appears to reduce the problem relating to the value of the out-of plane

stress at low Poisson's ratio.

Two different SRI methods have been considered in conjunction with 4-node quadrilateral elements in the computation of bearing capacity. The G, K split was found to give marginally better results than the λ, μ split and is to some extent a more logical subdivision of the deviatoric and volumetric terms. Reduced integration suffered from hourglassing whereas full integration resulted in 'locking' and gave unconservative results. With SRI, generally good results were obtained, however the effectiveness of the method with frictional soils was improved by the use of an associated flow rule. As has often been observed in the past, the computation of bearing capacity and numerical convergence in general was found to become considerably more arduous for friction angles over 30°.

Although the results from the 3-d analyses have not been thoroughly presented here for reasons of space, good agreement has been observed between the 8-node brick element with SRI as compared with results obtained using meshes of higher order elements such as the 20- and 14-node bricks. Work continues on the study of bearing capacity of circular and rectangular footings.

ACKNOWLEDGMENT

This research has been supported by grant from the UK Science and Engineering Research Council (SERC GR/G 55921).

REFERENCES

1. Zienkiewicz, O.C., Humpheson, C. and Lewis, R.W. (1975) "Associated and non-associated viscoplasticity and plasticity in soil mechanics", Geotechnique 25, No 4, 671-689

2. Griffiths, D.V. (1982) "Computation of bearing capacity factors using finite element", Geotechnique 32, No 3, 195-202

3. Sloan, S.W. and Randolph, M.F. (1982) "Numerical prediction of collapse loads using finite element methods", Int. J. Numer. Analyt. Meth. Geomech., Vol 6, 47-76

4. de Borst, R. and Vermeer, P.A. (1984) "Possibilities and limitations of finite elements for limit analysis", Geotechnique 34, No 2, 199-210

5. Prevost, J.H. and Hughes, T.J.R. (1981) "Finite element solution of elastic-plastic boundary value problems", J. Appl. Mech., ASME, Vol 48, No 1, 69-74

6. Hughes, T.J.R. (1987) "The Finite Element Method. Linear Static and Dynamic Finite Element Analysis", Prentice- Hall, Englewood Cliffs

7. Nagtegaal, J.C., Parks, D.M. and Rice, J.R. (1974) "On numerically accurate finite element solutions in the fully plastic range", Comp. Meth. Appl. Mech. Engng., Vol 4, 153-177

8. Mase, G.E. (1970) "Theory and Problems of Continuum Mechanics", Schaum's Outline Series, McGraw-Hill, New York

9. Mok, F.B. and Griffiths, D.V. (1993) "An assessment of Backward and Forward Euler methods applied to the Prandtl problem", Computational Mechanics in UK, Swansea

10. Crisfield, M.A. (1987) "Plasticity computations using the Mohr Coulomb yield criterion", Engineering Computations, Vol 4, 300-308

11. de Borst, R. (1987) "Integration of plasticity equations for singular yield functions", Computers and Structures, Vol 26, No 5, 823-829

12. Smith, I.M. and Griffiths, D.V. (1988) "Programming the Finite Element Method", 2nd ed., Wiley

13. Griffiths, D.V. (1989) "Computation of collapse loads in geomechanics by finite elements", Ingenieur-Archiv, Vol 59,237- 244